The FEBS Journal

FEBS PRESS science publishing by scientists

STRUCTURAL SNAPSHOT

The architecture of the 10-23 DNAzyme and its implications for DNA-mediated catalysis

Jan Borggräfe[1,2], Christoph G. W. Gertzen[3], Aldino Viegas[4,5], Holger Gohlke[3,6] and Manuel Etzkorn[1,2,7]

1 Institute of Physical Biology, Heinrich Heine University Düsseldorf, Germany
2 Institute of Biological Information Processing (IBI-7: Structural Biochemistry), Forschungszentrum Jülich, Germany
3 Institute for Pharmaceutical and Medicinal Chemistry, Heinrich Heine University Düsseldorf, Germany
4 UCIBIO, Department of Chemistry, NOVA School of Science and Technology, Universidade NOVA de Lisboa, Caparica, Portugal
5 Associate Laboratory i4HB – Institute for Health and Bioeconomy, NOVA School of Science and Technology, NOVA University Lisbon, Caparica, Portugal
6 Institute for Bio- and Geosciences (IBG-4: Bioinformatics), Forschungszentrum Jülich, Germany
7 Jülich Center for Structural Biology (JuStruct), Forschungszentrum Jülich, Germany

Keywords
10-23 DNAzyme; DNAzymes; MD; NMR

Correspondence
H. Gohlke, Institute for Pharmaceutical and Medicinal Chemistry, Heinrich Heine University Düsseldorf, Universitätsstr. 1, 40225 Düsseldorf, Germany
Tel: +49-211-81-13662
E-mail: gohlke@uni-duesseldorf.de and
M. Etzkorn, Institute of Physical Biology, Heinrich Heine University Düsseldorf, Universitätsstr. 1, 40225 Düsseldorf, Germany
Tel: +49-211-81-12023
E-mail: manuel.etzkorn@hhu.de

Present address
J. Borggräfe, Institute of Structural Biology, Molecular Targets and Therapeutics Center, Helmholtz Zentrum München, Neuherberg, 85764, München, Germany and Department of Chemistry, Bavarian NMR Center, Technical University of Munich, Garching, 85748, München, Germany

(Received 22 September 2022, revised 18 November 2022, accepted 5 December 2022)

doi:10.1111/febs.16698

Understanding the molecular features of catalytically active DNA sequences, so-called DNAzymes, is essential not only for our understanding of the fundamental properties of catalytic nucleic acids in general, but may well be the key to unravelling their full potential via tailored modifications. Our recent findings contributed to the endeavour to assemble a mechanistic picture of DNA-mediated catalysis by providing high-resolution structural insights into the 10-23 DNAzyme (Dz) and exposing a complex interplay between the Dz's unique molecular architecture, conformational plasticity, and dynamic modulation by metal ions as central elements of the DNA catalyst. Here, we discuss key features of our findings and compare them to other studies on similar systems.

Abbreviations
6-thio-G, 6-thio-2′-deoxyguanosine; CSP, chemical shift perturbations; Dz, variant of the 10-23 DNAzyme targeting the PrP mRNA; EPR, electron paramagnetic resonance; MBS, metal-ion binding sites; MD, molecular dynamics; NMR, nuclear magnetic resonance; PRE, paramagnetic relaxation enhancement.

Introduction

Identified almost 30 years ago by *in vitro* selection, DNAzymes are single-stranded DNA oligomers with catalytic activity [1–4]. One of the most prominent DNAzymes is the RNA-cleaving 10-23 DNAzyme (Dz), which is among the most catalytically active DNA-sequences [2,5]. Dz consists of two variable substrate-binding arms that can hybridise with a complementary RNA target, and a catalytic loop of 15 nucleotides, which cleaves the RNA target in an Mg^{2+}-dependent manner (Fig. 1A). The substrate-binding arms can be varied in length and sequence to allow specific binding to virtually any RNA of interest with high selectivity, entailing a substantial therapeutic and biotechnological potential. For instance, DNAzyme-based therapies could be applied to reduce expression levels of disease-related proteins, such as those involved in cancer, viral diseases or neurodegenerative diseases [6–13]. Yet, DNAzymes often underperform in a cellular environment [3,14–16], obstructing many therapeutic and biotechnological applications. While randomised and/or systematic optimisation led to noticeable improvements during the last decades [16–23], only accurate mechanistic insights will open the door for complementary rational-design approaches that could provide new angles to overcome the persisting limitations of the system. The crystal structures of the RNA-cleaving DNAzyme 8-17 [24] and the RNA-ligating 9DB1 DNAzyme [25] were two important contributions in this respect. While early

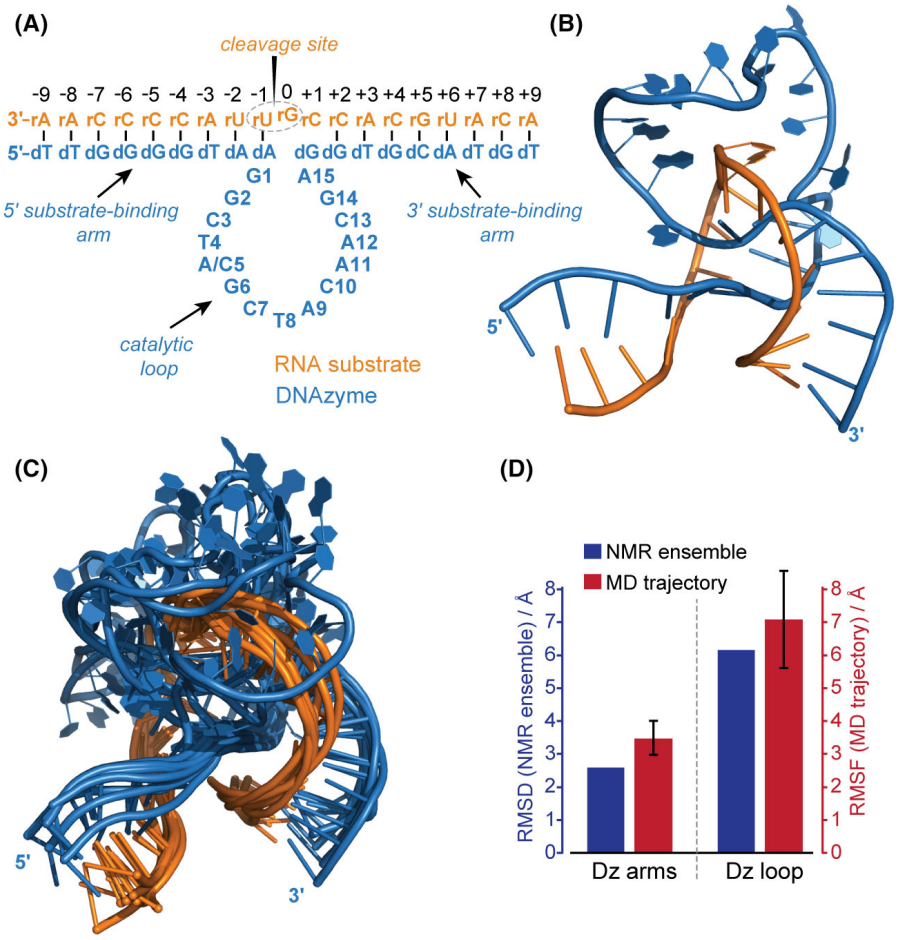

Fig. 1. Overview of the Dz's structural features. (A) Schematic representation of the used Dz (blue) and RNA (orange) sequence and numbering. While the original sequence of Dz contains an adenine at position 5 of the catalytic loop, our structural studies focused on a variant containing a cytosine mutation (A5C). This variant shows improved NMR-spectroscopic properties and is active, albeit at lower rates. (B) One representative structure from the NMR ensemble of the precatalytic Dz:RNA complex (the Dz's loop region is shown with explicit nucleobase representation). (C) Overlay of all seven structures of the NMR ensemble (PDB: 7PDU) showing elevated levels of structural plasticity in the loop region. Structural representations in (B, C) were prepared using PYMOL [51]. (D) Comparison between calculated (pair-wise) RMSD values of the NMR ensemble for nucleotides in the arm and the loop region (blue) and root-mean-square fluctuations (RMSF) obtained for the respective regions in MD simulations (red). Error bars represent the standard error of the mean over 10 simulation replicas.

attempts to determine the structure of Dz resulted in catalytically irrelevant crystallographic artefacts [26], we recently determined the solution structure of Dz [27]. In our study, we applied a combination of nuclear magnetic resonance (NMR) spectroscopy, molecular dynamics (MD) simulations, electron paramagnetic resonance (EPR), and other biophysical and biochemical assays to obtain atomistic and time-resolved mechanistic insights into the Dz-mediated catalysis. Unless stated otherwise, the results discussed in this structural snapshot will refer to this publication [27].

Discussion

Unravelling the architecture of the 10-23 DNAzyme

During the catalytic cycle, a DNAzyme adopts different states with differential structural features, including a single-stranded conformation and the Dz:RNA complex in a pre- or post-catalytic state. Using a combination of conventional and real-time NMR methodology, we identified distinct features of all apparent states and detected transient intermediate states pointing to rate-limiting steps of the catalytic cycle.

Arguably, one of the most important conformational states of the catalytic cycle is the precatalytic Dz:RNA complex in the presence of Mg^{2+}. Here, the RNA substrate is bound to the Dz in an activatable conformation. Our study confirmed that a 2′-fluorine substitution at the cleavage site (rG_0) locks the precatalytic state, allowing prolonged data acquisition in the presence of various concentrations of Mg^{2+} and other metal ions, while not affecting the overall structure of the complex.

Applying an array of conventional and novel NMR methods, such as ^{19}F-derived distance restraints, paramagnetic relaxation enhancement (PRE), residual dipolar couplings and exact NOEs (nuclear Overhauser effect), we were able to determine a structural ensemble of the precatalytic Dz:RNA complex (PDB code: 7PDU) (Fig. 1B,C). Furthermore, we identified distinct regions showing pronounced metal-ion interactions, which will be discussed in more detail below. One of the most remarkable features of the obtained structure is a condensed core region involving an additional turn of the Dz's loop around the RNA substrate. This was an unexpected but very exciting finding, since this fold appears effective in simultaneously locking the substrate in place and exposing the cleavage site to specific regions of the catalytic loop.

Our structural insights are predominantly based on NMR experiments and MD simulations, yielding a structural ensemble with a moderate overall resolution that characterises the conformational space sampled by the Dz instead of a high-resolution snapshot of one single conformation, for example, trapped in a cleavage-competent state with fixed interatomic distances and molecular geometries. While this introduces ambiguities in distinct structural features, our data suggest that the obtained ensemble and conformational plasticity may well represent the intrinsic features of the precatalytic Dz:RNA complex in solution at physiologically relevant temperature and buffer conditions.

To gain further insights into the structural integrity and possible modes of action, we carried out MD simulations of the Dz:RNA complex in integrative modelling using the AMBER suite of molecular simulation programmes [28]. The MD trajectories reveal, on the one hand, that the overall fold of the precatalytic Dz:RNA complex is stable over the simulation time of 1 μs and, on the other hand, identify regions in Dz that exhibit increased conformational fluctuations. Both the NMR and MD data consistently indicate that the magnitude of the Dz's structural plasticity strongly varies along its sequence with a rather conserved structure of the two substrate binding arms and increased plasticity in the loop region (Fig. 1D). To illustrate the sampled conformational space, a movie depicting one MD trajectory of the Dz:RNA complex over a simulation time of 1 μs is provided here: https://doi.org/10.25838/d5p-37.

The identified fold together with the Dz's conformational plasticity point to a central mechanistic feature, that is, the alignment of the substrate in the centre of the Dz' catalytic loop and the exposition of the RNA cleavage site to distinct nucleotides. Our data show that the cleavage site is effectively locked by the Dz, exhibiting the lowest conformational plasticity. Furthermore, the cleavage site is directly exposed to the 3′-side of the Dz's catalytic loop, which, on the contrary, displays the highest conformational plasticity. This arrangement likely promotes (transient) interactions of different functional groups of the Dz with the substrate moieties at the cleavage site, while the site can still be brought into a (temporally) stable 'cleavable' conformation. As discussed below, the interplay between loop and cleavage site is further modulated by (divalent) metal ions, which interact transiently with the precatalytic Dz:RNA complex, generating a highly dynamic interaction network.

Interestingly and in contrast to other DNAzymes, a characteristic feature of the 10-23 DNAzyme is the apparent absence of stable base pairing in its catalytic loop. Still, the 10-23 DNAzyme is considered one of the most active RNA-cleaving DNAzymes [5]. Thus, the highly dynamic interaction network observed for Dz appears to be a comparatively effective scaffold for

DNA catalysts, which originated from *in vitro* selection of rather short sequences comprising natural DNA nucleotides. However, our data also suggest that Dz, under the applied near-physiological buffer conditions, predominantly samples catalytically inactive conformations that only transiently transition into catalytically active conformations. It can therefore be speculated that short sequences comprising the four standard DNA nucleotides used in most *in vitro* selection assays are likely not suited to build an optimal scaffold to catalyse RNA transesterification. While this points to a general limitation of the current DNAzyme technology, it also emphasises strategies that can overcome these limitations via rational or systematic usage of non-standard and/or non-native building blocks [16,17,29].

In general, the observed central link between the Dz's activity, conformational plasticity and dynamic exchange processes induced by metal-ion cofactors are strongly influenced by the applied measurement environments. This underlines the importance of appropriate measurement methodologies and conditions for DNAzyme studies. Furthermore, the observed level of conformational freedom that facilitates the conformational sampling of inactive structures also points to appealing new targets for the rational design of improved DNAzyme variants via the designated elimination of catalytically unfavourable 'off-pathway' conformations.

Deep-dive into the role of metal ions

To unravel the role of metal-ion cofactors in Dz-mediated catalysis, we carried out a comprehensive array of dedicated experiments and simulations. Overall, we identified different effects of metal ions that we relate to structural scaffolding, activation and catalysis.

Scaffolding

NMR-titration experiments with Mg^{2+}, Mn^{2+} and $Co(NH_3)_6^{3+}$ using the fluorine-stabilised precatalytic complex identified three metal-ion binding sites (Fig. 2A, MBS I–III). The strongest and largest binding area is located at the crossing of the Dz's binding arms (MBS I). Our data suggest that this binding site aims to counter the electrostatic repulsion arising from the dense packing of the negatively charged phosphate backbones of the crossing arms. $Co(NH_3)_6^{3+}$, a mimic for hexahydrated Mg^{2+}, shows clear binding to this site, pointing towards an outer-sphere interaction of the metal ions with the DNA/RNA backbones.

Mg^{2+} binding was also investigated using MD simulations. Previous MD simulations of DNAzymes used crystallographic information about the positions of Mg^{2+} ions for the starting structure [30,31]. By contrast, as such detailed information was missing in our case, we placed hexahydrated, octahedrally coordinated Mg^{2+} at a distance to the DNAzyme structure and allowed them to diffuse into it, leading to local charge compensation. We showed previously that this allows an effective equilibration of the system [32]. Still an important step of our MD simulation studies was to extend the thermalisation procedure of the simulation system and the relaxation of restraints sixfold compared to other simulations [30] to enable sufficient metal-ion diffusion (see reference [33] for more details). These MD simulations corroborated the binding sites and provided insight into the likelihood of mechanistic features.

Our NMR data and MD simulations show that Mg^{2+} binding stabilises and condenses the complex, a process we termed 'scaffolding'. It should be noted that, in general, a conventional NMR-based structure calculation will be biased towards the shortest distances in an ensemble. Hence, it is not surprising that the obtained structure is in a condensed conformation already at low Mg^{2+} concentrations, and it cannot be excluded that parts of the native ensemble may also be in a more open conformation under these conditions.

Interestingly, a DNA:RNA complex comprising the same nucleotide sequences but lacking the catalytic core only shows a diffuse metal-ion interaction pattern over the whole sequence, missing the defined binding site I identified for the same nucleotides in the Dz:RNA complex (Fig. 2B,C). This demonstrates that the metal-ion interactions in this area are not merely unspecific but, likely, a direct requirement for the scaffolding, which is initiated by the nucleotides of the catalytic loop. It is further likely that also monovalent ions can, at least partly, fulfil the role of Mg^{2+} in MBS I (*vide infra*).

From a structural point of view, the condensation is possible by the *syn* conformation of the nucleotides at position −1 and an out-of-register flip of dG_{+1} that breaks the expected Watson–Crick pairing, making room for the unique passage of the loop through the otherwise double helix of the arms (Fig. 2D).

Activation

MBS II is located at the 5′-side of the loop, and Mg^{2+}-binding in this site will lead to larger structural rearrangements of this region. Interestingly, only loop positions 1–3, 5 and 6 showed significant effects for Mn^{2+} binding, indicative of a specific divalent metal-ion binding site. The importance of O6 and N7 of the

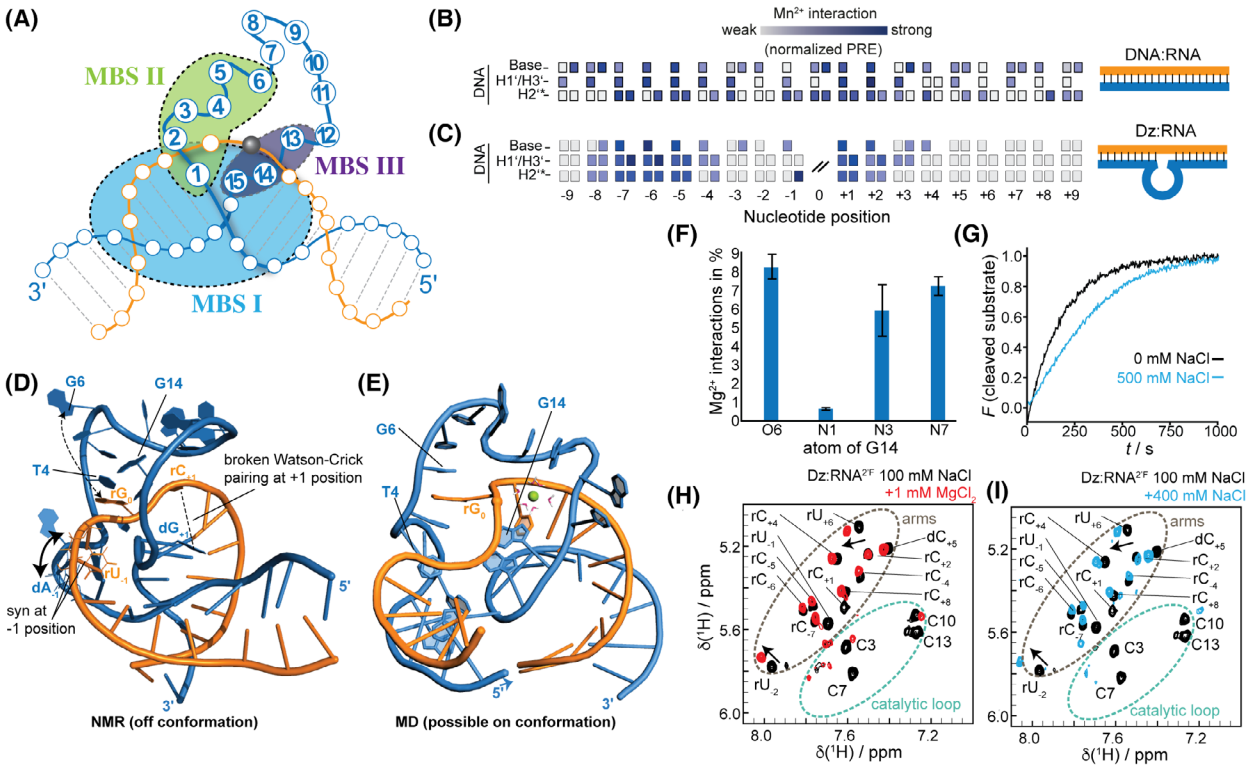

Fig. 2. Structural details and effects of metal-ion interactions. (A) Schematic illustration of the three metal ion binding sites (MBS I–III) found in the Dz:RNA complex. (B). Mn^{2+}-induced PRE rates (as probes for direct interactions) in a conventional DNA:RNA double helix comprising the identical sequence of the Dz arm region but lacking the catalytic loop. A diffuse binding pattern along the full sequence is observed. (C) Same data as in (B) but for the arm regions of the Dz:RNA complex showing the formation of distinct binding regions (predominantly representing MBS I). (D) Illustration of central nucleotides and features of the structure shown in Fig. 1B. The respective structural features and experimental conditions are most consistent with a conformation that underwent scaffolding but not conformational activation. (E) Snapshot of the MD simulations displaying a potentially cleavage-competent conformation. A hydrated Mg^{2+} in proximity to the cleavage site is also shown (green sphere). (F) Propensity of interactions of different functional groups of G14 with Mg^{2+} occurring during the MD simulations. Error bars represent the standard error of the mean over 10 simulation replicas. Structural representations in (D, E) were prepared with PYMOL [51]. (G) Single turnover cleavage assay of Dz in the presence of 1 mM Mg^{2+} and indicated concentrations of Na^+ (data taken from [49]). (H, I) NMR fingerprint spectra of precatalytic Dz:RNA complexes under indicated conditions. (H) Changing the $MgCl_2$ concentration from 0 to 1 mM leads to chemical shift perturbations (CSPs) in the arm region and peak disappearance in the loop region. While the CSPs are indicative of fast exchanging interactions and/or structural rearrangements, the disappearance of NMR peaks is indicative of interactions in a slower time regime (intermediate exchange), pointing to stronger Mg^{2+} interactions in the loop region. Interestingly, very similar effects are found when changing the NaCl concentration from 100 to 500 mM (I, blue, in the absence of Mg^{2+}). Panels B,C,G,H,I combine and reproduce data reported in Refs [27,49].

Guanine at position 6 (G6) was already identified [34,35], and we could confirm the relevance of the 6-oxo group of G6 in our Dz variant via a 6-thio substitution that strongly reduces Mg^{2+}-induced activity. Previous studies further showed that G1, G2 and T4 could be exchanged by an abasic nucleotide or a C3 spacer with only low activity loss [36], suggesting that functionally relevant metal-ion binding in MBS II is either promoted by the phosphate backbone or that the metal ion is required to restructure an inactive conformation of the nucleobase regions.

We showed that T4 undergoes an Mg^{2+}-induced flip-out that may act as a molecular switch during activation. Changing T4 to any other nucleotide will strongly reduce activity [34], which may indicate that larger nucleobases cannot act as a similar switch due to steric hindrance or unfavourable interactions. Another study using thiophosphate identified the importance of metal-ion binding to the phosphate between T4 and A5 [35]. This interaction may be facilitated by the observed flip-out of T4. Noteworthy, the restraints for the NMR structure determination were obtained on a Dz variant containing an A5C variation in the loop and at a Mg^{2+} concentration of 1 mM, which is well below the saturation concentration of the Mg^{2+} interaction of this variant at MBS II. Consequently, the obtained structural

ensemble should be dominated by the 'off-conformation'.

Our data obtained on the original A5 Dz variant reveals that the mutation likely does not alter the overall structure of the precatalytic complex. However, distinct chemical shift perturbations between the A5 and C5 Dz variants are also found that support a structural link connecting the mutation site (i.e. MBS II) with distinct nucleotides on the other side of the loop (i.e. MBS III), and the cleavage site. While this highlights a connection between the Dz's central elements, it does not allow, at the moment, to extract detailed structural consequences. Still, a very important difference induced by the A5C mutation can be clearly identified, which is a considerably reduced Mg^{2+} binding affinity (specific to MBS II) as well as differential Mg^{2+} association/dissociation rates. In this respect, the stronger Mg^{2+} binding and, in particular, also the slower exchange rate found for the original A5 Dz variant (related to longer Mg^{2+} occupation times in MBS II) may well lead to an increased population of active conformations and consequently explain the higher activity of the A5 variant.

Our MD data show that G6 engages in π-π stacking interactions with rG_0, suggesting that this interaction, together with the NMR-observed distinct binding features in MBS II, causes a rearrangement of the Dz's catalytic loop and the RNA-cleavage site into a cleavage-competent state (Fig. 2E), a process we termed 'conformational activation'.

Overall, it is tempting to speculate that T4 acts as an Mg^{2+}-triggered molecular switch that, in the 'on-conformation', promotes π-π stacking of G6 with rG_0. This stacking interaction subsequently supports the formation of the so-called 'in-line attack conformation' at the cleavage site, which is a prerequisite for the transesterification reaction.

Catalysis

MBS III is located at the more flexible 3′-side of the loop. Contrary to the other metal-ion binding sites, more distinct Mg^{2+}-induced CSPs were detected, indicative of binding without substantial structural alterations. MBS III is also characterised by strong PRE effects due to Mn^{2+} binding, especially for nucleotides C13, G14 and A15. Previous studies identified the 6-oxo group of G14 and the 6-amino group of C13 as essential for Dz's function [34,35]. While functional groups of A15 do not seem to be essential for catalysis [4,27], introducing an intercalator between A15 and dN_{+1} improves activity [37]. The stacking interactions between A15, dN_{+1}, and the intercalator probably stabilise the active conformation as well as the out-of-register flip of dG_{+1}, which we experimentally detected due to the absence of characteristic NMR correlations to its 3′ neighbour. In this respect, note that dG_{+1} was the only nucleotide of the arm region for which these peaks were expected but clearly absent in the spectrum, substantially corroborating its out-of-register flip. In line with the resulting absence of stable base pairing of dG_{+1} with its RNA counterpart, any mutation at position +1 leaves the Dz functional, but purines seem to be slightly more active, which is in line with a potential stacking interaction between A15 and dG_{+1}.

Our MD simulations detect interactions between G14 and O2′ of rG_0 during 3.3% of the sampling time, rendering G14 an apparent key component for catalysis. For the 8-17 DNAzyme and the Hammerhead ribozyme, it is suggested that deprotonated guanine-N1 acts as a Brønsted base extracting a proton from the cleavage site's O2′, followed by an in-line attack of O2′ at the phosphate [24] (Fig. 3). Our data are well in line with G14 of Dz having a similar role in catalysis. To act as an efficient proton acceptor, it has also been observed in ribozymes that the pK_a of N1 of the catalytic Guanine is lowered by metal-ion interaction with N7 [38], pointing to a potentially similar functional role of Mg^{2+} binding in MBS III of Dz.

However, metal-ion binding sites of nucleic acids often have redundant proton donors/acceptors that allow different binding modes [39]. The elevated structural plasticity observed for the Dz's nucleotides in MBS III will not only allow, but likely also promote, different metal-ion interactions (Fig. 2F). In this picture, it is likely that only a subset of the possible interactions is favourable for catalysis, while other interactions may be detrimental for activity, for example, by blocking and/or competing with active conformations. Using a 6-thio substitution at G14, which reduces Mg^{2+} interaction while maintaining Mn^{2+} interactions of this moiety in Dz, we could show that Mg^{2+}- but not Mn^{2+}- mediated activity is considerably increased. This strongly points to catalytically unfavourable Mg^{2+} interactions in the conventional 6-oxo-G14 variant, which may be one source limiting the Dz's activity.

Recently, an L-platform has been identified in the 8-17 DNAzyme and ribozymes [40]. This L-platform describes a characteristic arrangement of nucleobases in the catalyst and the substrate's cleavage site. The arrangement primes a catalytic guanine by keeping it in a position to attack the O2′ of the substrate as the general base. This involves base stacking of the catalytic guanine being sandwiched between the N-1

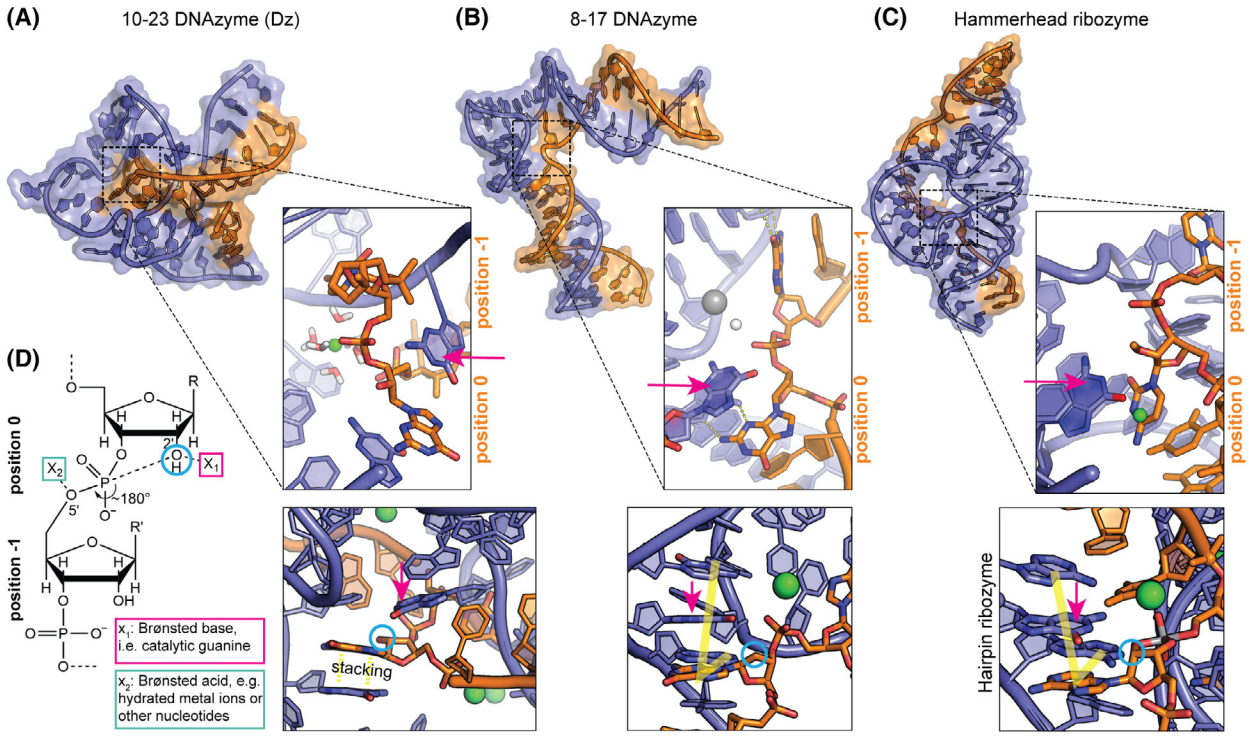

Fig. 3. Comparison of different RNA-cleaving systems. (A) 10-23 DNAzyme (PDB: 7PDU, inlets show snapshot from MD simulation), (B) 8-17 DNAzyme (PDB: 5XM8), (C) hammerhead ribozyme (PDB: 3ZP8, top panels) and hairpin ribozyme (PDB: 1M5O [41], lower panel). DNA and RNA (substrate) are coloured blue and orange respectively. Structural representations in A–C were prepared using PYMOL [51]. (D) Schematic of the cleavage site in an 'in-line-attack conformation' (i.e. O2′-P-O5′ showing an approx. 180° angle). Key positions for an acid–base mechanism are indicated (x_1, x_2). While the overall structures of the systems differ, the architecture of the respective cleavage sites generally promotes a similar acid–base mechanism involving a guanine at the catalytic centre serving as Brønsted base (pink arrow in inlets A, B and C) that is capable of abstracting the 2′H at the substrate nucleotide position '0' (highlighted by a cyan circle in A–D). Metal ions are in (A) Mg^{2+} (green), in (B) Pb^{2+} (grey), in (C) Na^{+} (green) and water molecules depicted as sticks (A, MD data) or white sphere (B, crystallographic data). The lower inserts highlight the L-platform identified in the 8-17 DNAzyme (B) and the hairpin ribozyme (C). A translucent 'L' marks the L-platform nucleotides. For Dz, 'L-platform' characteristic stacking interactions of the catalytic G14, its 5′-neighbouring nucleobase and the 5′-nucleotide of the cleavage site are neither found in the NMR ensemble nor in the MD simulations. Rather, the 5′-nucleobase of the cleavage site (position 0) is stabilised by stacking interactions with G6 of the catalytic loop (lower insert in A). Note that the here-used nucleotide numbering focuses on the Dz (Fig. 1A) and differs from an RNA/cleavage site-focused numbering. In the latter numbering, the highlighted positions '0' and '−1' will translate to '−1' and '+1' respectively.

nucleobase at the 5′-end of the scissile phosphate and the subsequent nucleobase at the 5′-end of the catalytic guanine. Furthermore, the nucleobase at the 3′-end of the catalytic guanine engages in base-pairing interactions with the nucleobase at the 5′-end of the scissile phosphate. Finally, adjacent nucleobases form a metal-ion binding pocket close to the catalytic guanine for the hydrated ion to act as a general acid (Fig. 3B,C lower insert). That way, the N1 of the catalytic guanine can attack the O2′, for example, in the hairpin ribozyme (Fig. 3C, lower insert) [41].

For Dz, neither the NMR ensemble nor the MD simulations reveal the characteristic stacking interactions of an L-platform arrangement. Rather, our data indicate that similar functional groups and mechanisms are in place but that they are acting in a different molecular framework. Generally, and in line with the L-platform, the N1 nitrogen of the catalytic guanine could be important for proton abstraction from the substrate's O2′ when this atom is in the in-line attack conformation [24,42]. For Dz, our MD data identify Mg^{2+} close to G14, specifically, atoms O6, N3 and N7 (Fig. 2F). While our 6-thio-G14 modification indicates that the interactions with O6 are detrimental to activity, our data would be well in line with a pK_a reduction induced by Mg^{2+} binding to N7 of G14, promoting an attack of N1 to the substrate's O2′.

In the precatalytic Dz:RNA complex, the RNA substrate is kinked at the cleavage site, orienting the arms at an angle of approximately 120° towards each other

(Fig. 3A), which was recently also observed in atomic force microscopic studies [43]. This feature is likewise found in other RNA-cleaving nucleic acid systems such as the 8-17 DNAzyme [24] (Fig. 3B), Hammerhead ribozyme (Fig. 3C) [44], Leadzyme [45] or HDV ribozyme [46]. One can speculate that this overall arrangement of the arms facilitates a local alignment of the in-line attack conformation at the cleavage site (O5′ of rG_0, and P and O2′ of rU_{-1} at approximately 180°). While the local alignment is stabilised by base pairing at the cleavage site in the 8-17 DNAzyme [24] and Hammerhead ribozyme [46], it is most likely stabilised by the π-π interaction between rG_0 and G6 in Dz. Noteworthy, similar stacking interactions have also been observed for the ligation junction in the RNA-ligating 9DB1 DNAzyme in the post-catalytic state [25].

To gain further insights into the Dz's mode of action, future MD studies may consider (a) the use of molecular solvation theory to predict water and metal ion binding sites in nucleic acids [47] or (b) treating the catalytic centre at the quantum mechanical level while using a molecular mechanics representation of the rest of the system or (c) using a deprotonated catalytic base to represent the state of attack better [30,31,48]. However, these methods generally work best in conjunction with an X-ray crystal structure of the DNAzyme that includes co-crystallised metal ions at the catalytic centre.

The interplay of different metal-ions

We observed that the structural effects of Mg^{2+} binding to the individual MBSs of Dz are saturated at concentrations below the saturation point of our kinetic assays. This is in line with a cooperative binding behaviour of divalent metal ions to the different MBSs, which is also observed in ITC, EPR and kinetic assays [14,49]. Accordingly, it is conceivable that scaffolding via binding to MBS I may promote conformational activation via binding to MBS II, and that occupation of MBS I and MBS II is a requirement for the catalytic role of Mg^{2+} in MBS III. In this respect, the relevant cleavage-competent structural features (i.e. G6 – rG_0 stacking, G14 interactions with O2′ of rG_0, and formation of the in-line attack conformation) were found more often in MD simulations when MBS II is occupied by hexahydrated Mg^{2+}.

In general, it can be anticipated that cooperative effects and binding of divalent metal ions to the different MBSs will also be influenced by the presence of monovalent ions. Interestingly, our previous studies showed that NaCl and KCl had no effect on the binding cooperativity when analysed by ITC, but Mg^{2+} binding affinities were reduced by half [49]. We could confirm this effect via NMR-based characterisations and show that NaCl can partly reproduce the effects of $MgCl_2$ (Fig. 2H,I). From this data, we propose that monovalent ions can essentially mimic the effects of divalent ions at MBS I and possibly also MBS II. Consequently, monovalent ions should generally be able to induce scaffolding and conformational activation of the Dz:RNA complex. For the Hammerhead ribozyme, it was observed that very high concentrations of monovalent ions can also promote catalysis in the absence of divalent metal ions, and crystallographic studies of the system revealed that Na^+ occupies similar binding sites as Mg^{2+} also involving O6 of the general base G12 [44]. However, so far, no catalytic activity of Dz has been reported in the absence of divalent metal ions, even at high monovalent ion concentrations [49]. These findings again point to an additional role of divalent metal ions in catalysis that most likely involves MBS III. This would also be in line with the observed inhibiting effects of NaCl binding [49] to MBS III that could displace potentially functionally important Mg^{2+} ions.

Inhibiting effects induced by $Co(NH_3)_6^{3+}$ (demonstrated in [27]) that mimics hexahydrated Mg^{2+}, as well as differential effects observed for Mn^{2+} and Mg^{2+} (demonstrated in [49]), further suggest that inner-sphere contacts of the functionally relevant metal ions may also play a role in catalysis.

So how many and what kind of metal ions are ultimately required for Dz-mediated catalysis? While our data do not allow quantifying the exact metal-ion occupancy at the time of substrate cleavage, conclusions related to this question can still be drawn from our data and the manifold complementary studies. However, first, one should be aware that the question itself may be misleading, since it assumes that only one distinct occupation results in an active conformation. Yet, our data suggest different binding interactions of metal ions within MBS I that also include occupation by more than one metal ion at a time. Furthermore, one metal ion may also be shared between the different MBSs, for example, by MBS II and MBS III. When bringing the observed dynamic exchange processes and structural plasticity into this picture, it also appears possible that the metal-ion induced conformations will remain 'intact' for some time after the metal ion has already left its DNA/RNA interaction partners. This could particularly be the case for the scaffolding and, partly, also the conformational activation step, which will require larger conformational rearrangements.

In general, our MD and NMR data indicate that metal ion-induced structural effects require molar ratios (Mg^{2+}:Dz) of well above 10 to be saturated. While it is unlikely that all metal ions interact simultaneously, it should be emphasised that when the Dz cleaves its substrate RNA, differential occupation scenarios with metal ions are well conceivable.

It can further be speculated that the absence of a not strictly defined metal ion binding pattern, and consequently the absence of a 'rigid-switch' that is inherent to many enzymes, will obstruct a fast transition between an active precatalytic and inactive postcatalytic conformation. In this speculative picture, for example, dissociation of a catalytically relevant metal ion may not directly lead to an inactive structural scaffold of the postcatalytic Dz:RNA complex. Being still in a conformation that allows proton transfer from/to the RNA, this could foster a potential back reaction resulting in rate-limiting intermediate states that would also be consistent with our time-resolved NMR insights.

Conclusions and consequences

DNA catalysts are fascinating systems that, on the one hand, offer the opportunity to better understand fundamental properties of one of the most central molecules of life and, on the other hand, carry an enormous potential for biotechnological and therapeutic applications [50].

Our results contributed to developing a mechanistic understanding of the system, which in combination with numerous complementary breakthroughs in the field, identified central features that are important for function and/or pose limitations for (cellular) applications. As to the latter, it appears that low levels of free intracellular Mg^{2+} in combination with the identified low Mg^{2+} affinities of all three MBSs, as well as potential detrimental effects of higher cellular levels of Na^+/K^+, constitute a challenging 'working environment' for the Dz [3,14,49]. Our structural insights further suggest that the Dz's activity is limited by the combination of a high level of structural plasticity and the manifold interaction possibilities DNA nucleotides have to offer, resulting in a fast and transient sampling of a large number of different active and inactive conformations. This view may also hint at why randomised and/or systematic optimisations using natural nucleotides have only led to slow progress over the last decades. Excitingly, the dynamic picture of DNAzymes and their transient interactions with their environment also opens new avenues for rational-design strategies introducing (non-natural) chemical modifications, which are tailored to reduce detrimental interactions and/or stabilise functionally relevant conformations. We are therefore confident that, fuelled by a better mechanistic understanding, new generations of DNAzymes may soon become attractive means for manifold biotechnological and therapeutic applications.

Acknowledgements

The authors acknowledge access to the Jülich-Düsseldorf Biomolecular NMR Center. HG is grateful for computational support and infrastructure provided by the 'Zentrum für Informations- und Medientechnologie' (ZIM) at the Heinrich Heine University Düsseldorf and the John von Neumann Institute for Computing (NIC) (user ID: HKF7, VSK33). We thank Hannah Rosenbach for providing activity data. This work was supported by the German Research Foundation (DFG) (103/4-1, ET 103/4-3, and the Heisenberg grant ET 103/5-1) to ME, the Volkswagen Foundation to ME and HG (project no. 9B798) and the European Union's Horizon 2020 research and innovation program under the Marie Skłodowska-Curie grant agreement no. 660258 to AV. Open Access funding enabled and organized by Projekt DEAL.

Conflict of interest

The authors declare no conflict of interest.

Author contributions

All authors participated in interpretations of available results and writing this article.

References

1 Breaker RR, Joyce GF. A DNA enzyme that cleaves RNA. *Chem Biol*. 1994;**1**:223–9.
2 Santoro SW, Joyce GF. A general purpose RNA-cleaving DNA enzyme. *Proc Natl Acad Sci USA*. 1997;**94**:4262–6.
3 Silverman SK. Catalytic DNA: scope, applications, and biochemistry of deoxyribozymes. *Trends Biochem Sci*. 2016;**41**:595–609.
4 Rosenbach H, Victor J, Etzkorn M, Steger G, Riesner D, Span I. Molecular features and metal ions that influence 10-23 DNAzyme activity. *Molecules*. 2020;**25**:3100.
5 Hollenstein M. DNA catalysis: the chemical repertoire of DNAzymes. *Molecules*. 2015;**20**:20777–804.
6 Dass CR. Deoxyribozymes: cleaving a path to clinical trials. *Trends Pharmacol Sci*. 2004;**25**:395–7.

7 Khachigian LM. Deoxyribozymes as catalytic nanotherapeutic agents. *Cancer Res*. 2019;**79**:879–88.
8 Krug N, Hohlfeld JM, Kirsten AM, Kornmann O, Beeh KM, Kappeler D, et al. Allergen-induced asthmatic responses modified by a GATA3-specific DNAzyme. *N Engl J Med*. 2015;**372**:1987–95.
9 Fokina AA, Stetsenko DA, François JC. DNA enzymes as potential therapeutics: towards clinical application of 10-23 DNAzymes. *Expert Opin Biol Ther*. 2015;**15**:689–711.
10 Zhang N. DNAzyme as a rising gene-silencing agent in theranostic settings. *Neural Regen Res*. 2022;**17**:1989–90.
11 Zhang N, Bewick B, Schultz J, Tiwari A, Krencik R, Zhang A, et al. DNAzyme cleavage of CAG repeat RNA in polyglutamine diseases. *Neurotherapeutics*. 2021;**18**:1710–28.
12 Potaczek DP, Unger SD, Zhang N, Taka S, Michel S, Akdağ N, et al. Development and characterization of DNAzyme candidates demonstrating significant efficiency against human rhinoviruses. *J Allergy Clin Immunol*. 2019;**143**:1403–15.
13 Huo W, Li X, Wang B, Zhang H, Zhang J, Yang X, et al. Recent advances of DNAzyme-based nanotherapeutic platform in cancer gene therapy. *Biophys Rep*. 2020;**6**:256–65.
14 Victor J, Steger G, Riesner D. Inability of DNAzymes to cleave RNA in vivo is due to limited Mg^{2+} concentration in cells. *Eur Biophys J*. 2018;**47**:333–43.
15 Young DD, Lively MO, Deiters A. Activation and deactivation of DNAzyme and antisense function with light for the photochemical regulation of gene expression in mammalian cells. *J Am Chem Soc*. 2010;**132**:6183–93.
16 Taylor AI, Wan CJK, Donde MJ, Peak-Chew S-Y, Holliger P. A modular XNAzyme cleaves long, structured RNAs under physiological conditions and enables allele-specific gene silencing. *Nat Chem*. 2022;**14**:1295–305.
17 Wang Y, Nguyen K, Spitale RC, Chaput JC. A biologically stable DNAzyme that efficiently silences gene expression in cells. *Nat Chem*. 2021;**13**:319–26.
18 Liu C, Chen Y, Zhao J, Wang Y, Shao Y, Gu Z, et al. Self-assembly of copper–DNAzyme nanohybrids for dual-catalytic tumor therapy. *Angew Chem Int Ed Engl*. 2021;**60**:14324–8.
19 Wang Y, Liu E, Lam CH, Perrin DM. A densely modified M^{2+} –independent DNAzyme that cleaves RNA efficiently with multiple catalytic turnover. *Chem Sci*. 2018;**9**:1813–21.
20 Schubert S, Gül DC, Grunert H-P, Zeichhardt H, Erdmann VA, Kurreck J. RNA cleaving "10-23" DNAzymes with enhanced stability and activity. *Nucleic Acids Res*. 2003;**31**:5982–92.
21 Paul S, Wong AAWL, Liu LT, Perrin DM. Selection of M^{2+} – independent RNA-cleaving DNAzymes with side-chains mimicking arginine and lysine. *Chembiochem*. 2022;**23**:e202100600.
22 Huang PJ, Liu J. In vitro selection of chemically modified DNAzymes. *ChemistryOpen*. 2020;**9**:1046–59.
23 Chakravarthy M, Aung-Htut MT, Le BT, Veedu RN. Novel chemically-modified DNAzyme targeting integrin alpha-4 RNA transcript as a potential molecule to reduce inflammation in multiple sclerosis. *Sci Rep*. 2017;**7**:1613.
24 Liu H, Yu X, Chen Y, Zhang J, Wu B, Zheng L, et al. Crystal structure of an RNA-cleaving DNAzyme. *Nat Commun*. 2017;**8**:2006.
25 Ponce-Salvatierra A, Wawrzyniak-Turek K, Steuerwald U, Höbartner C, Pena V. Crystal structure of a DNA catalyst. *Nature*. 2016;**529**:231–4.
26 Nowakowski J, Shim PJ, Prasad GS, Stout CD, Joyce GF. Crystal structure of an 82-nucleotide RNA-DNA complex formed by the 10-23 DNA enzyme. *Nat Struct Biol*. 1999;**6**:151–6.
27 Borggräfe J, Victor J, Rosenbach H, Viegas A, Gertzen CGW, Wuebben C, et al. Time-resolved structural analysis of an RNA-cleaving DNA catalyst. *Nature*. 2022;**601**:144–9.
28 Case DA, Cheatham TE, Darden T, Gohlke H, Luo R, Merz KM, et al. The Amber biomolecular simulation programs. *J Comput Chem*. 2005;**26**:1668–88.
29 Freund N, Taylor AI, Arangundy-Franklin S, Subramanian N, Peak-Chew S-Y, Whitaker AM, et al. A two-residue nascent-strand steric gate controls synthesis of 2′-O-methyl- and 2′-O-(2-methoxyethyl)-RNA. *Nat Chem*. 2022. https://doi.org/10.1038/s41557-022-01050-8
30 Ekesan Ş, York DM. Dynamical ensemble of the active state and transition state mimic for the RNA-cleaving 8-17 DNAzyme in solution. *Nucleic Acids Res*. 2019;**47**:10282–95.
31 Aranda J, Terrazas M, Gómez H, Villegas N, Orozco M. An artificial DNAzyme RNA ligase shows a reaction mechanism resembling that of cellular polymerases. *Nat Catal*. 2019;**2**:544–52.
32 Hanke CA, Gohlke H. Ligand-mediated and tertiary interactions cooperatively stabilize the P1 region in the guanine-sensing riboswitch. *PLoS One*. 2017;**12**:e0179271.
33 Gertzen CGW, Gohlke H. Molecular modeling and simulations of DNA and RNA: DNAzyme as a model system. *Methods Mol Biol*. 2022;**2439**:153–70.
34 Zaborowska Z, Fürste JP, Erdmann VA, Kurreck J. Sequence requirements in the catalytic core of the "10-23" DNA enzyme. *J Biol Chem*. 2002;**277**:40617–22.
35 Nawrot B, Widera K, Wojcik M, Rebowska B, Nowak G, Stec WJ. Mapping of the functional phosphate

groups in the catalytic core of deoxyribozyme 10-23. *FEBS J*. 2007;**274**:1062–72.
36 Wang B, Cao L, Chiuman W, Li Y, Xi Z. Probing the function of nucleotides in the catalytic cores of the 8-17 and 10-23 DNAzymes by abasic nucleotide and C3 spacer substitutions. *Biochemistry*. 2010;**49**:7553–62.
37 Asanuma H, Hayashi H, Zhao J, Liang X, Yamazawa A, Kuramochi T, et al. Enhancement of RNA cleavage activity of 10-23 DNAzyme by covalently introduced intercalator. *Chem Commun*. 2006;5062–4.
38 Sigel RKO, Pyle AM. Alternative roles for metal ions in enzyme catalysis and the implications for ribozyme chemistry. *Chem Rev*. 2007;**107**:97–113.
39 Schnabl J, Sigel RK. Controlling ribozyme activity by metal ions. *Curr Opin Chem Biol*. 2010;**14**:269–75.
40 Gaines CS, Piccirilli JA, York DM. The L-platform/L-scaffold framework: a blueprint for RNA-cleaving nucleic acid enzyme design. *RNA*. 2020;**26**:111–25.
41 Rupert PB, Massey AP, Sigurdsson ST, Ferré-D'Amaré AR. Transition state stabilization by a catalytic RNA. *Science*. 2002;**298**:1421–4.
42 Cortés-Guajardo C, Rojas-Hernández F, Paillao-Bustos R, Cepeda-Plaza M. Hydrated metal ion as a general acid in the catalytic mechanism of the 8-17 DNAzyme. *Org Biomol Chem*. 2021;**19**:5395–402.
43 Mao D, Li Q, Li Q, Wang P, Mao C. A conformational study of the 10–23 DNAzyme via programmed DNA self-assembly. *Chem Commun*. 2022;**58**:6188–91.
44 Anderson M, Schultz EP, Martick M, Scott WG. Active-site monovalent cations revealed in a 1.55-Å-resolution hammerhead ribozyme structure. *J Mol Biol*. 2013;**425**:3790–8.
45 Wedekind JE, McKay DB. Crystal structure of the Leadzyme at 1.8 Å resolution: metal ion binding and the implications for catalytic mechanism and allo site ion regulation. *Biochemistry*. 2003;**42**:9554–63.
46 Ke A, Zhou K, Ding F, Cate JHD, Doudna JA. A conformational switch controls hepatitis delta virus ribozyme catalysis. *Nature*. 2004;**429**:201–5.
47 Giambaşu GM, Case DA, York DM. Predicting site-binding modes of ions and water to nucleic acids using molecular solvation theory. *J Am Chem Soc*. 2019;**141**:2435–45.
48 Ekesan Ş, York DM. Who stole the proton? Suspect general base guanine found with a smoking gun in the pistol ribozyme. *Org Biomol Chem*. 2022;**20**:6219–30.
49 Rosenbach H, Borggräfe J, Victor J, Wuebben C, Schiemann O, Hoyer W, et al. Influence of monovalent metal ions on metal binding and catalytic activity of the 10–23 DNAzyme. *Biol Chem*. 2020;**402**:99–111.
50 Micura R, Höbartner C. Fundamental studies of functional nucleic acids: aptamers, riboswitches, ribozymes and DNAzymes. *Chem Soc Rev*. 2020;**49**:7331–53.
51 Schrödinger L. The {PyMOL} molecular graphics system, version 2.5.2; 2015.